Volume 13, Number 2, 2020. pp. 157-163

Jordan Journal of Physics

ARTICLE

Structural, Electrical and Thermal Properties of Composites Based on Conducting Polymer

N. Aribou[a], **S. Barnoss**[a], **M. El Hasnaoui**[a], **M. E. Achour**[a] and **L. C. Costa**[b]

[a] *Laboratory of Material Physics and Subatomic, Faculty of Sciences, Ibn Tofail University, BP 242, 14000 Kenitra, Morocco.*

[b] *I3N and Physics Department, University of Aveiro, 3810-193 Aveiro, Portugal.*

Doi : https://doi.org/10.47011/13.2.7

Received on: 08/08/2019; *Accepted on: 3/11/2019*

Abstract: In this work, we report the structural, thermal and electrical properties of composites consisting of polypyrrole particles in a polymethylmethacrylate matrix. Electrical resistivity analysis of these percolating composites showed a remarkable change in the conduction mechanisms below and above the percolation threshold. Structural properties were studied using X-ray diffraction, showing increases in the crystallinity index for filler concentrations above the critical percolation. Thermogravimetric analysis was used to study thermal degradation. It shows a transition from a single peak for concentrations below the percolation threshold to a double peak for concentrations above that point. The increase in the degradation temperature with the concentration of polypyrrole indicates the increase of thermal stability.

Keywords: Conducting polymer, Percolation threshold, Crystallinity, Thermal degradation, X-Ray diffraction.

Introduction

Conducting polymers are the purpose of many types of research, not only at the fundamental level, but also as several potential applications [1-4]. These materials can combine the electrical properties of the filler with the mechanical properties of the matrix. The description of the mechanisms of electronic transport of these composites is based on the concept of percolation [5]. Percolating systems based on composite materials are formed with insulating matrix loaded with conducting charges. One of the most important conducting polymers is polypyrrole (PPy); it exhibits interesting properties, such as high conductivity and can easily mix with a polymeric matrix [6]. On the other hand, polymethylmethacrylate (PMMA) is a suitable matrix, because it is readily available and easy to cast into desired forms maintaining the mechanical integrity of the matrix.

A study of the electrical and dielectric properties of PMMA/PPy composite has been already presented. El Hasnaoui et al. [7] analyzed the electrical conductivity spectrum, finding that the hopping of charge carriers between localized states is the dominant conduction mechanism. Aribou et al. [8] performed an analysis on the real and imaginary parts of permittivity in a wide range of frequency using the impedance spectroscopy, concluding that the response of these materials has an abnormal low-frequency dispersion due to the localized or almost free charge carriers. Thus, in order to complete these studies, the thermal and structural properties of these composites were investigated. In this paper, we explore experimental measurements on such composites

Corresponding Author: Mohamed El Hasnaoui **Email**: med.elhasnaoui@uit.ac.ma

in order to obtain the structure, electrical resistivity and thermal properties characterizing the electrical transport mechanisms governing this type of material.

Experimental

Samples Preparation

The PPy powder was obtained by doping intrinsic PPy with tosylate anion TS^-. The doping rate was controlled by the XPS technique and was found of the order of one sulphur (S) for four nitrogen (N); that is, one tosylate ion TS^- for four pyrrole monomers [9]. The average grain size of PPy is in the range of 10–15 µm. The two powders, PMMA and PPy, were mixed in several proportions of filler and pressed at 5000 $kg.cm^{-2}$ and 150 °C. Then, the samples were allowed to cool freely to room temperature to give solid disc-shaped samples. All discs had a diameter of 13 mm and 3-4 mm thickness. The direct current conductivities of the PPy and PMMA matrix are, respectively, 54 and 3.10^{-8} $(\Omega.m)^{-1}$ and the densities are 1.20 and 1.14-1.20 $g.cm^{-3}$, respectively. The glass transition temperature of PMMA polymer is $T_g \approx 115$ °C [5].

Characterization

Structural characterizations were made by X-ray diffraction (XRD) using a Philips X'pert MPD diffractometer, operating at 40 kV and 30 mA, equipped with a Cu anticathode of wavelength $\lambda = 1.5406$ Å.

The electrical resistivity was measured using a 617 Keithley electrometer, at constant temperature T=300 K. The samples were prepared as discs of thickness of about 3-4 mm with aluminum electrodes of 10 mm diameter on the opposite sides of the sample. The electrical contacts were made with silver paint.

TGA was carried out using a Shimadzu TGA-50 Thermogravimetric Analyzer. The measurements were taken under an atmosphere of nitrogen with a flow rate of 30 $mL.min^{-1}$, at temperatures between 20 and 800 °C and a heating rate of 5 $°C.min^{-1}$. The samples were placed in platinum cells.

Results and Discussion

X-ray Diffraction

X-ray diffraction (XRD) diagrams of four samples of the PMMA/PPy composites are shown in Fig. 1. It allows us to make an analysis of the dispersion of the PPy inclusions in the PMMA matrix. The diffraction peak that is observed at 31.2° corresponds to conducting filler that is the TS^--doped PPy structure. The peak intensity increases with PPy concentration, which means that the crystallinity of the PMMA/PPy composite increases. The crystallinity index (CrI) was calculated from XRD data according to the Segal empirical method [10] written as follows:

$$CrI = \left[\left(I_f - I_s\right)/I_f\right] \times 100 \quad (1)$$

where I_f is the intensity of both crystalline and amorphous peak corresponding to PPy-doped TS^- particles at $2\theta = 31.2^\circ$ and I_s is the minimum height between two peaks at about $2\theta = 26^\circ$. The crystallinity index (CrI) of PMMA/PPy composites has been calculated for all concentrations of PPy particles by taking the amorphous and crystalline contributions to the diffraction intensity and the results are shown in Fig. 2. As can be seen, the obtained values of CrI are between 40 and 70 % which are greater than those obtained in two series: PMMA/CdS composites that are between 39 and 42 % [11] and PMMA/TiO_2 composites that are between 10 and 19 % [12]. These differences are related to the type of conducting charges used in each series; i.e., the PPy doped with TS^- has more effect on PMMA crystallinity than cadmium sulfide (CdS) and titanium dioxide (TiO_2) semiconductor particles. It can also be noticed that there is a significant change in the value of the crystallinity index below and above the percolation threshold, which will be determined into "electrical resistivity analysis" section. Above the percolation threshold, the crystalline index takes the highest value, which demonstrates the significant effect of PPy particles on electrical transport mechanisms governing this conducting composite.

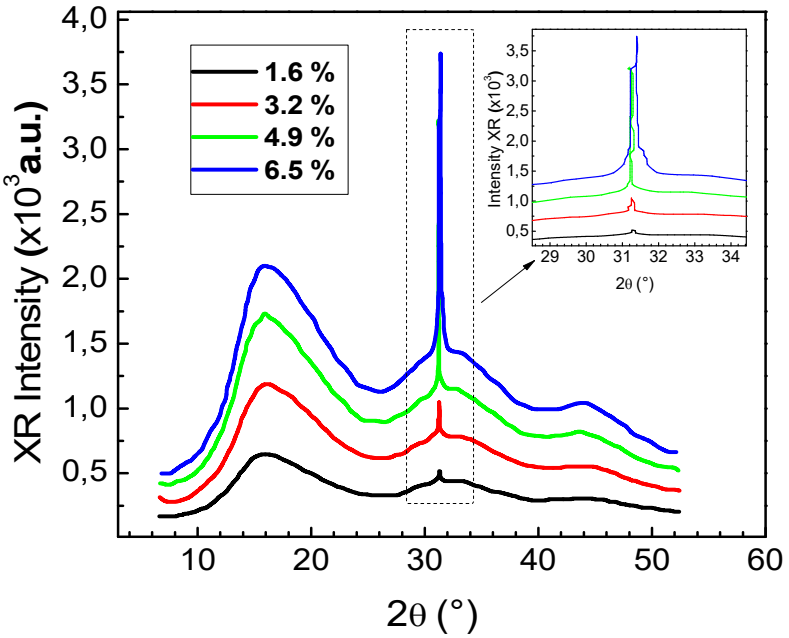

FIG. 1. X-ray diffraction (XRD) diffractograms of PMMA/PPy composites.

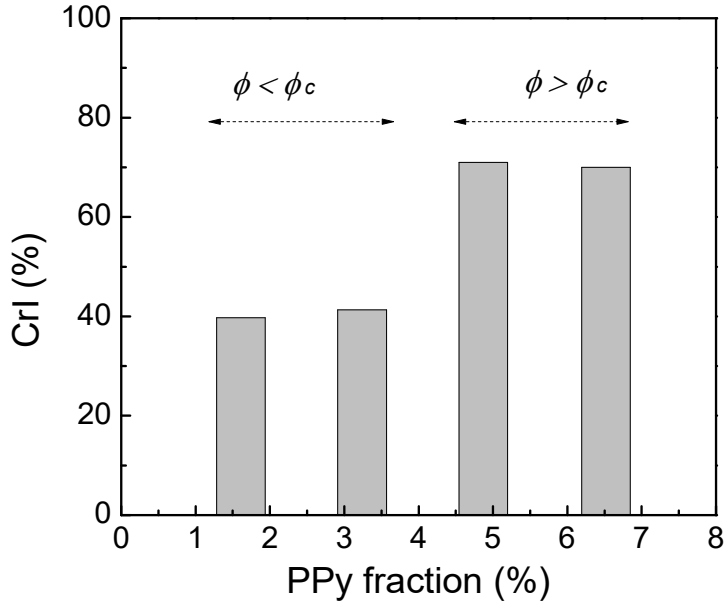

FIG. 2. The crystallinity index (CrI) as a function of PPy concentration at a temperature of 300 K.

Electrical Resistivity Analysis

Fig. 3 shows the semi-logarithmic curve of ρ as a function of PPy fraction embedded in a PMMA polymer matrix, at a temperature of T=300 K. As can be seen, the behavior of ρ can be divided into three regions [13]. In region I, the small decrease in resistivity of the composite can be attributed to the transportation of the small number of conducting charges through the PMMA/PPy composite without having any continuous conductive path. In region II, resistivity decreases sharply due to a continuous conductive path developed in the PMMA matrix. The estimated percolation threshold, ϕ_c, is about 3.24%, where resistivity begins to decrease abruptly. This major jump in resistivity could be attributed to the formation of an infinite agglomerate pathway that allows electrons to travel a macroscopic distance through the PMMA matrix. In region III, further addition of conducting particles has a marginal effect on resistivity. The creation of PPy conducting network-like structure in the PMMA/PPy

composites results in removing the static charge from the sample surface [14]. The behavior of experimental data, in this region, could be modelled by the percolation model [15,16] written as follows:

$$\rho = \rho_o(\phi - \phi_c)^{-t} \text{ for } \phi > \phi_c \quad (2)$$

where, the exponent t is a parameter related to the dimensionality of the composite and ρ_o is a pre-exponent factor. Fig. 4 shows $log\rho$ as a function of $\log(\phi - \phi_c)$ for the PPy fractions above the percolation threshold. Fitting the percolation model (Eq. (2)) to the experimental data yields the pre-exponent $\rho_o = 34{,}7\ (\Omega.m)$ and $t = 1.69 \pm 0.12$. This value is close to that of the universal three-dimensional percolating systems that is equal to 2 [17]. Omastov and Simon [14] have presented a study on the same composites. finding the same behavior, but with a lower percolation threshold. This can be justified by the prepared procedure, where they used a dilution with 25% of water, containing $FeCl_3$ particles. In our case, the composites contain TS^- anions, changing the viscosity of the PMMA/PPy composite. It is known that low percolation thresholds are always achieved with low viscosity composites [18] and could be also the result of the degree of dispersion or interfacial adhesion between PPy particles and the PMMA matrix [19].

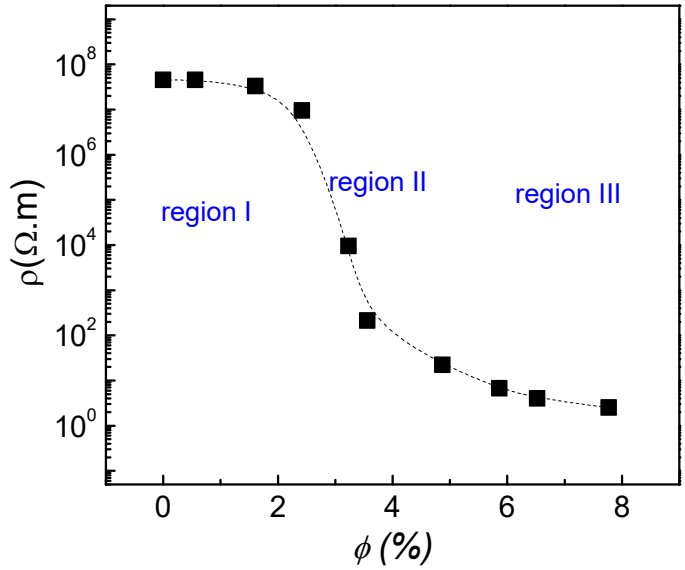

FIG. 3. Semi-log plot of electrical resistivity ρ *versus* PPy concentration at room temperature. Dashed line is drawn to guide the eyes.

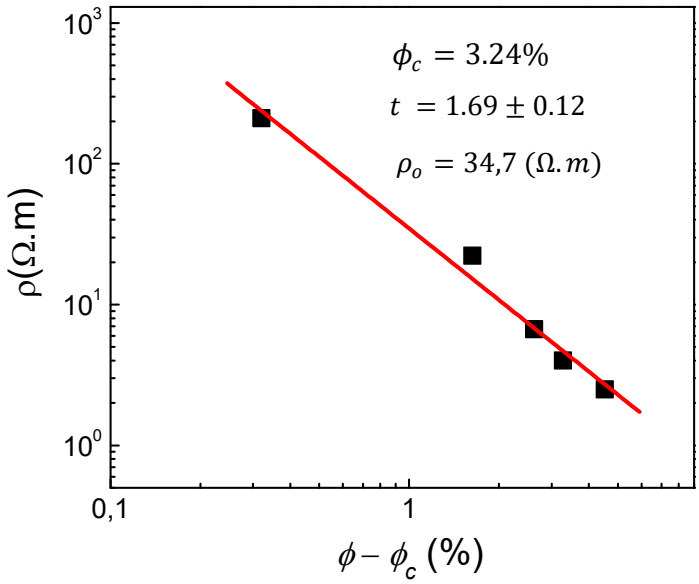

FIG. 4. Log-log plot of ρ *versus* $\phi - \phi_c$ for concentrations above the percolation threshold at a temperature of T = 300 K. Solid line represents the best linear fit of data with a correlation coefficient $R^2 = 0.98$.

Thermal Properties

We have reported in Fig. 5 the measured relative evolution of the mass losses of four samples obtained from the TGA spectrum in the range of temperature from 20 to 500 °C. It is clearly seen that the thermal degradation of these samples starts around 250 °C with a significant mass loss of approximately 97%, corresponding to thermal degradation of the PMMA polymer. The loss of mass reaches its maximum value beyond 440 °C for a given PPy concentration and the rate of degradation slightly depends on the PPy fraction in the matrix. In order to look for deep analysis and identify the significant variations of these curves, we calculated the derivative weight of each curve. Figs. 6 and 7 show the comparative curves of weight loss and its derivatives for the PPy fraction-reinforced PMMA matrix. The thermal decomposition temperatures of the PMMA/PPy composites increased with increasing the concentration of PPy. The presence of the PPy particles can lead to the stabilization of the PMMA matrix and good interfacial adhesion between the PPy and the PMMA may restrict the thermal motion of the PMMA molecules [20], resulting in increased thermal stability of the PMMA/PPy composites.

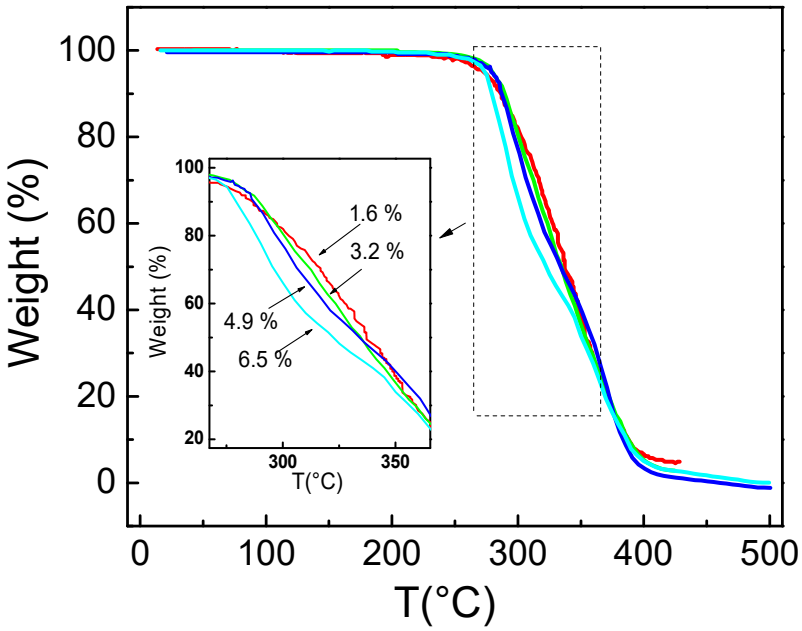

FIG. 5. TGA thermograms of PMMA/PPy composites for different PPy concentrations.

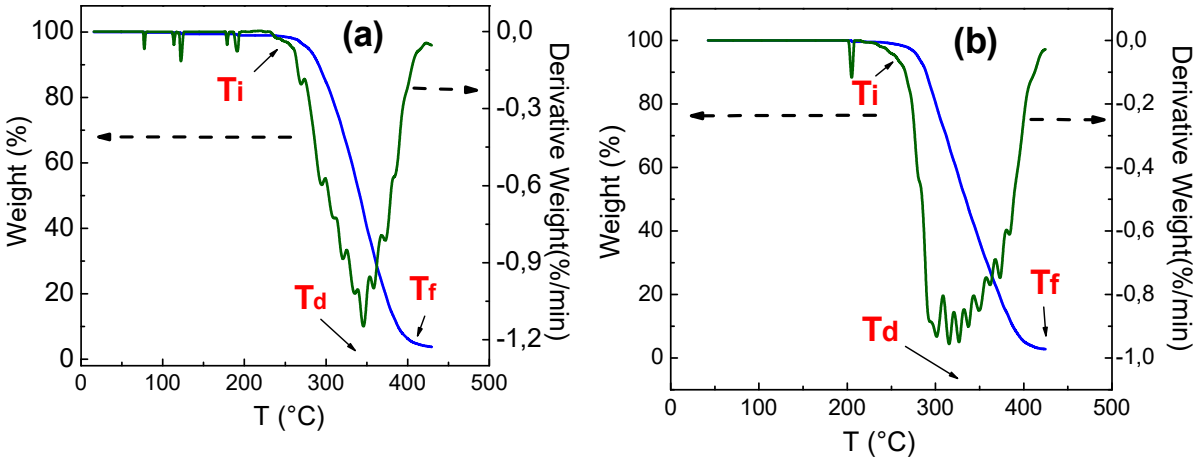

FIG. 6. TGA and derivative thermograms of PMMA/PPy composites for PPy concentrations below the percolation threshold, 1.6 % (a) and 3.2 % (b).

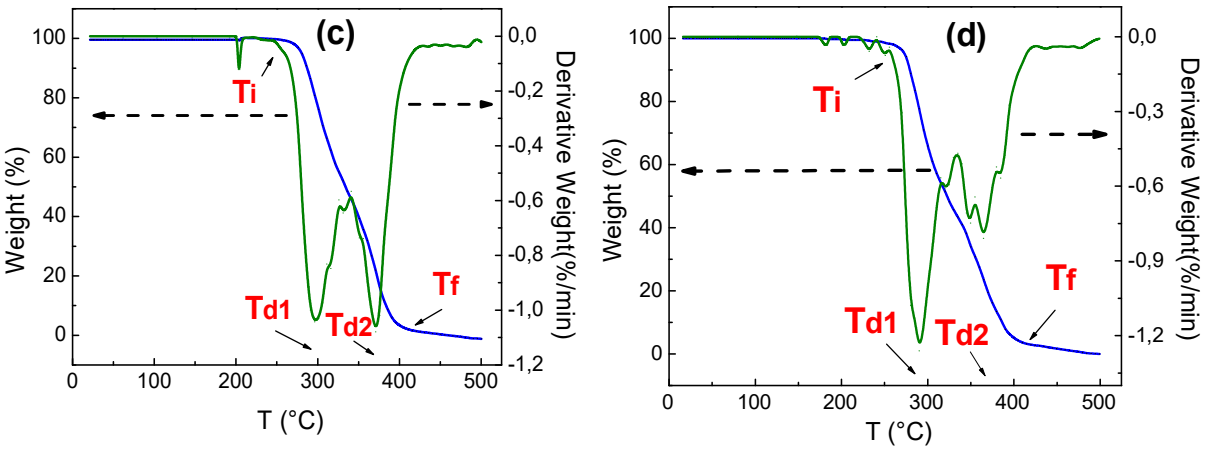

FIG. 7. TGA and derivative thermograms of PMMA/PPy composites for PPy concentrations below the percolation threshold, 4.9 % (c) and 5.6 % (d).

It clearly appeared from Table 1 that, for concentrations below the percolation threshold ϕ_c (Fig. 6), there is only a single endothermic peak in derivative weight, whereas there are double endothermic peaks for concentrations above ϕ_c (Fig. 7). Table 1 illustrates the temperature values of initial degradation T_i, first degradation T_{d1}, second degradation T_{d2} and final degradation T_f. We observe that there are significant changes in the values of these parameters; i.e., when the PPy filler increases from low concentrations ($\phi < \phi_c$) to high concentrations ($\phi > \phi_c$), the temperature of initial degradation (243-245 °C) is increased to (253-254 °C) and the degradation of PMMA/PPy follows two steps, characterizing two thermal degradations. We attribute this behavior to the existence of two non-compatible phases forming the molecular level of composites that explains the phenomenon of degradation found below and above the percolation threshold. The same behavior was observed in thermal analysis of PMMA/multiwalled carbon nanotube (MWCNT) composites presented by Choi et al. [21], where they found that the addition of MWNTs as a filler improved the intrinsic properties.

TABLE 1. Temperature and mass loss characteristics of thermal degradation of PMMA/PPy composites.

ϕ (%)	1.6	3.2	4.9	6.5
T_i (°C)	243	245	254	253
T_{d1} (°C)	345	327	297	290
T_{d2}(°C)			370	365
T_f(°C)	405	408	405	403
Mass of loss (step I) (%)			49	48
Mass of loss (step II) (%)	95	96	48.5	48.5
Mass of loss			97.5	96.5

Conclusion

This paper presents a study of structural, electrical and thermal properties of PPM/PPy composites. Analysis of electrical resistivity *versus* PPy fraction showed a percolation threshold at which the behavior of transport mechanism changes. Thermal gravimetric analysis was used to study the evolution of the thermal stability of PMMA/PPy composites; it shows that the rate of degradation slightly depends on the PPy content in the PMMA matrix. Moreover, X-ray diffraction patterns indicate that the crystallinity index of composites increases with increasing the PPy fraction.

References

[1] Chandrasekhar, P., "Conducting Polymers, Fundamentals and Applications: Including Carbon Nanotubes and Graphene", 2nd Ed., (Cham Switzerland: Springer International Publishing, 2018), pp. 549-714.

[2] Deshpande, P.P. and Sazou, D., "Corrosion protection of metals by intrinsically conducting polymers", 1st Ed., (CRC Press LLC, New York, 2016).

[3] Otero, T.F., Schneider, H.J. and Shahinpoor, M., "Conducting-polymers: bioinspired intelligent materials and devices", (Croydon U.K.: Royal Society of Chemistry, 2015).

[4] Bouknaitir, I., Aribou, N., Elhad Kassim, S.A., El Hasnaoui, M., Melo, B.M.G., Achour, M.E. and Costa, L.C., Spectro. Lett., 50 (2017) 196.

[5] Achour, M.E., Droussi, A., Zoulef, S., Gmati, F., Fattoum, A., Belhadj, M.A. and Zangar, H., Spectro. Lett., 41 (2008) 328.

[6] Costa, L.C., Henry, F., Valente, M.A., Mendiratta, S.K. and Sombra, A.S., Eur. Polym. J., 38 (2002) 1495.

[7] El Hasnaoui, M., Abazine, K., Achour, M.E. and Costa, L.C., J. Optoelectron. Adv. Mater., 18 (2016) 389.

[8] Aribou, N., Elmansouri, A., Achour, M.E., Costa, L.C., Belhadj, M.A., Oueriagli, A. and Outzourhit, A., Spectro. Lett., 45 (2012) 477.

[9] Belhadj, M.A., Miane, J.L. and Zangar, H., Polym. Int., 50 (2001) 773.

[10] Segal, L., Creely, J.J., Martin Jr., A.E. and Conrad, C.M., Textile Res. J., 29 (1959) 786.

[11] Patel, A.K., Jain, N., Patel, P., Das, K. and Bajpai, R., AIP Conference Proceedings, 1942 (2018) 070029.

[12] El-Zaher, N.A., Melegy, M.S. and Guirguis, O.W., Natural Science, 6 (2014) 859.

[13] Foulger, S.H., J. Appl. Polym. Sci., 72 (1999) 1573.

[14] Omastov, M. and Simon, F., J. Mater. Sci., 35 (2000) 1743.

[15] Stauffer, D. and Aharony, A., "Introduction to percolation theory", (Taylor and Francis, London, 1992).

[16] Kirkpatrick, S., Rev. Mod. Phys., 45 (1973) 574.

[17] Grimaldi, C and Balberg, I., Phys. Rev. Lett., 96 (1) (2006) 066602.

[18] Kovacs, J.Z., Velagala, B.S., Schulte, K. and Bauhofer, W., Compos. Sci. Technol., 67 (2007) 922.

[19] Ma, P.-C., Siddiqui, N.A., Marom, G. and Kim, J.K., Compos., Part A: Appl. Sci. Manuf., 41 (2010) 1345.

[20] El-Zaher, N.A., Melegy, M.S. and Guirguis, O.W., Natural Science, 6 (2014) 859.

[21] Choi, H.J., Lim, J.Y. and Zhang, K., Diamond Relat. Mater., 17 (2008) 1498.